Dynamics of the generalized Kuramoto model with nonlinear coupling: Bifurcation and stability

Wei Zou* and Jianwei Wang
School of Mathematical Sciences, South China Normal University, Guangzhou 510631, China

(Received 1 June 2020; accepted 13 July 2020; published 27 July 2020)

We systematically study dynamics of a generalized Kuramoto model of globally coupled phase oscillators. The coupling of modified model depends on the fraction of phase-locked oscillators via a power-law function of the Kuramoto order parameter r through an exponent α, such that $\alpha = 1$ corresponds to the standard Kuramoto model, $\alpha < 1$ strengthens the global coupling, and the global coupling is weakened if $\alpha > 1$. With a self-consistency approach, we demonstrate that bifurcation diagrams of synchronization for different values of α are thoroughly constructed from two parametric equations. In contrast to the case of $\alpha = 1$ with a typical second-order phase transition to synchronization, no phase transition to synchronization is predicted for $\alpha < 1$, as the onset of partial locking takes place once the coupling strength $K > 0$. For $\alpha > 1$, we establish an abrupt desynchronization transition from the partially (fully) locked state to the incoherent state, whereas there is no counterpart of abrupt synchronization transition from incoherence to coherence due to that the incoherent state remains linearly neutrally stable for all $K > 0$. For each case of α, by performing a standard linear stability analysis for the reduced system with Ott-Antonsen ansatz, we analytically derive the continuous and discrete spectra of both the incoherent state and the partially (fully) locked states. All our theoretical results are obtained in the thermodynamic limit, which have been well validated by extensive numerical simulations of the phase-model with a sufficiently large number of oscillators.

DOI: 10.1103/PhysRevE.102.012219

I. INTRODUCTION

Spontaneous synchronization is a universal cooperative phenomenon in large systems consisting of many interacting oscillatory units, which has long been an important issue of research in the fields of nonlinear dynamics, network science, and complex systems. Investigating the underlying mechanism of synchrony provides deep insights for understanding the macroscopic dynamics in diverse contexts of physics, chemistry, and biology [1–3]. The most successful paradigm for studying synchronization of coupled oscillators is the Kuramoto model introduced in 1975 [4], which has been used to explain the emergence of collective synchronization in many parts of science and technology [5–8], such as electrochemical oscillators [9], flashing fireflies [10], arrays of lasers [11,12], power grids [13–15], Josephson junctions [16,17], etc. Marvelously, the Kuramoto model turns out to be analytically tractable in the thermodynamic limit.

The Kuramoto model describes a collection of N phase oscillators, whose dynamics is governed by the following set of globally coupled first-order ordinary differential equations,

$$\dot{\theta}_j = w_j + \frac{K}{N}\sum_{k=1}^{N}\sin(\theta_k - \theta_j), \quad j = 1, 2, ..., N, \quad (1)$$

where θ_j is the phase of the jth oscillator, w_j is its natural frequency sampled according to a prescribed distribution function $g(w)$, and the parameter K controls the global coupling strength. To quantify the degree of coherence of system (1), the complex order parameter is generally defined as

$$R = re^{i\psi} = \frac{1}{N}\sum_{k=1}^{N} e^{i\theta_k}, \quad (2)$$

which is the centroid of N points $e^{i\theta_j}$ on the unit circle in the complex plane. The amplitude $0 \leqslant r \leqslant 1$ measures the phase coherence, and ψ gives the average phase. If all the oscillators are scattered roughly uniformly around the unit circle, then one has $r \approx 0$. However, if a large amount of oscillators are concentrated tightly, then $r \approx 1$; most of the oscillators seem to form a single giant clump. In the continuum limit of $N \to \infty$, Kuramoto developed a self-consistency approach to show that if $g(w)$ is unimodal and symmetric with respective to its center w_0, the second-order phase transition to synchronization is generically observed, where the partially synchronized (locked) state with a constant $r > 0$ bifurcates supercritically and continuously from the incoherent state with $r = 0$ at a critical coupling strength $K_c = 2/\pi g(w_0)$ [1]. Although Kuramoto's self-consistency analysis is ingenious and successful in identifying the steady solutions of his model in the infinite-N limit, it fails to reveal stability properties of the system dynamics. By linearizing the Fokker-Planck equation about the incoherent state, Strogatz and Mirollo obtained the first rigorous stability results for Kuramoto model [18]. Later, Mirollo and Strogatz continued to settle the issues of the linear stability of the fully and the partially synchronized states for the model [19,20]. In recent years, the stability analysis of both the incoherent and the partially locked states for the Kuramoto model has been justified in a more mathematically rigorous footing [21–25].

*weizou83@gmail.com

Another significant advance in the analytical description of macroscopic dynamics for the Kuramoto model has been made by Ott and Antonsen in their seminal works [26,27], where they presented an amazing ansatz that allows the asymptotic behavior of the model to be explored from a reduced low-dimensional system. After that, for past decades, the Ott-Antonsen ansatz has been served as a powerful tool to study dynamics of various variants of the Kuramoto model. Some examples of such studies include effects with symmetric (or asymmetric) rational frequency distributions [28–34], time delays [35–37], heterogeneous couplings [38–42], external forcing [43–46], chimera states [47–49], phase lag [50–53], etc. Recently, it has been further proved [54] that no loss of generality results in investigating both the existence and the linear stability of the partially locked states of Kuramoto model from the reduced system derived by Ott-Antonsen ansatz.

In this paper, we consider an extension of the Kuramoto model, where the global coupling is modified to depend on the number of synchronized oscillators via a power-law function of the Kuramoto order parameter r through an exponent $\alpha > 0$,

$$\dot{\theta}_j = w_j + \frac{Kr^{\alpha-1}}{N}\sum_{k=1}^{N}\sin(\theta_k - \theta_j), \tag{3}$$

which was first proposed by Filatrella, Pedersen, and Wiesenfeld in Ref. [55], suggested by experiments on arrays of coupled Josephson junctions, lasers, and mechanical systems. The coupling scheme in Eq. (3) can be deemed to be a minimal form of nonlinear coupling for Kuramoto-type model [56,57], which has also been extended to the Winfree model [58]. The model Eq. (3) with $\alpha = 1$ degenerates to the classic Kuramoto model, whereas $\alpha \neq 1$ produces the desired functional dependence of the coupling on the fraction of the phase-locked oscillators. With Kuramoto's self-consistency argument, the authors of Ref. [55] analytically predicted the value of r on the stable branch of partially locked states, where they confined their study to Lorentzian-distributed nature frequencies. However, they did not treat the other unstable branch of partially (fully) locked states when $\alpha > 1$, and did not carry out the stability analysis of their model. To the best of our knowledge, until now, both the detailed bifurcation diagrams of synchronization and the linear stability analyses of steady states for the modified model Eq. (3) are still missing.

The present work is devoted to filling the theoretical gaps of the generalized Kuramoto model with r-dependent coupling in Eq. (3). First, we show that synchronization diagrams of r versus K can be systematically constructed from two parametric expressions of the self-consistency equation for r, which well predict all branches of partially and fully locked states for general forms of $g(w)$. With the parametric approach, we illustrate synchronization diagrams of r versus K for different cases of α with $g(w)$ to be Lorentzian, uniform, and triangle frequency distributions, respectively. Then, we analytically work out the spectrum of both the incoherent and the partially (fully) locked states by carrying out linear stability analyses for the reduced system with Ott-Antonsen ansatz, from which their linear stability conditions are explicitly obtained. In what follows, we report our main results together with numerical simulations that validating our theoretical analyses.

II. THE MEAN-FIELD THEORY

By means of some simple manipulations, the model in Eq. (3) can be reformulated as the mean-field form of

$$\dot{\theta}_j = w_j + Kr^{\alpha}\sin(\psi - \theta_j). \tag{4}$$

Clearly, it can be seen that each oscillator is in fact coupled collectively through two macroscopic quantities r^{α} and ψ. The effective strength of the coupling in Eq. (4) is described by Kr^{α}. Due to the fact $r < 1$, the coupling is weakened for $\alpha > 1$ and strengthened if $\alpha < 1$ as compared with that of $\alpha = 1$. With the form in Eq. (4), it is convenient for us to apply Kuramoto's classical analysis to derive a self-consistency equation for the order parameter r. Throughout the paper, the frequency distribution $g(w)$ is taken to be unimodal and symmetric with respect to its center w_0. Note that by shifting to a frame rotating with frequency (i.e., $\theta \to \theta - w_0 t$), one may assume with no loss in generality that $g(w)$ has mean zero, i.e., $w_0 = 0$.

A. Continuum limit formulation

In the thermodynamic limit $N \to \infty$, the macroscopic dynamics of the generalized Kuramoto model in Eq. (3) can be described by a density function $f(\theta, w, t)$, which denotes a probability distribution of oscillators with phase θ at time t for a given frequency w. The density $f(\theta, w, t)$ satisfies the continuity equation of the form

$$\frac{\partial f}{\partial t} + \frac{\partial}{\partial \theta}(fv) = 0, \tag{5}$$

with the normalization condition

$$\int_0^{2\pi} f(\theta, w, t)d\theta = g(w) \tag{6}$$

for all w and t, where the phase velocity v is given by

$$\begin{aligned} v &= w + Kr^{\alpha}\sin(\psi - \theta) \\ &= w + K\mathrm{Im}(H(t)e^{-i\theta}) \\ &= w + \frac{K}{2i}[H(t)e^{i\theta} - H^*(t)e^{-i\theta}], \end{aligned} \tag{7}$$

with $H(t) = r^{\alpha}e^{i\psi}$, and the Kuramoto order parameter R defined in Eq. (2) takes the integral form of

$$R = re^{i\psi} = \int_{-\infty}^{+\infty}\int_0^{2\pi} e^{i\theta} f(\theta, w, t)d\theta dw. \tag{8}$$

Equations (5)–(8) form a closed description for the dynamics of Kuramoto-type systems of globally coupled phase oscillators Eq. (3) in the formal continuum limit of infinitely many oscillators $N \to \infty$.

B. Solutions of steady states

Our first task is to determine the steady solutions of Eq. (5) characterized by a density $f(\theta, w)$ and a velocity $v(\theta, w)$ independent of time t, for which both values of r and ψ are also time independent. Without loss of generality, one can set

$\psi = 0$ after an appropriate phase shift $\theta \to \theta - \psi$ if $\psi \neq 0$, which is due to the invariance of Eq. (3) under the global rotation. All stationary solutions of Eq. (5) satisfy

$$fv = C(w)g(w), \tag{9}$$

where $C(w)$ denotes the coefficient function depending only on w. One trivial stationary solution of Eq. (5) is

$$f_{\mathrm{IcS}}(\theta, w) = \frac{g(w)}{2\pi}, \tag{10}$$

which corresponds to the incoherent state with $r = 0$. Beside the incoherent state, the nontrivial stationary solutions of Eq. (5) with nonzero order parameter $r \neq 0$ given by

$$f_{\mathrm{PLS}}(\theta, w) = \begin{cases} \delta(\theta - \arcsin(\frac{w}{Kr^\alpha}))g(w) \text{ if } |w| \leqslant Kr^\alpha \\ \frac{\sqrt{w^2-(Kr^\alpha)^2}}{2\pi|w-Kr^\alpha \sin\theta|}g(w) \qquad \text{if } |w| > Kr^\alpha \end{cases} \tag{11}$$

correspond to the partially locked states with the first and second terms representing the densities of the locked and the drifting oscillators, respectively. Here $\delta(x)$ denotes the Dirac δ function. It can be seen that Eq. (11) consists of two distinct parts with heterogeneous and singular nature, which is in contrast to Eq. (10) for the incoherent state described by a smooth and constant density. Note that the density $f(\theta, w)$ of the fully locked states is given only by the first term of Eq. (11), in which $|w| \leqslant Kr^\alpha$ should be satisfied for all the oscillators.

The density of partially locked states in Eq. (11) can be derived as follows. By plugging $\psi = 0$ into Eq. (7), we get

$$\dot{\theta} = w - Kr^\alpha \sin\theta. \tag{12}$$

If $|w| \leqslant Kr^\alpha$, then Eq. (12) has the stable fixed point $\dot{\theta} = 0$ given by

$$\theta^* = \arcsin(\frac{w}{Kr^\alpha}), \quad \frac{\pi}{2} < \theta^* < \frac{\pi}{2}, \tag{13}$$

which leads to the first expression in Eq. (11) for the density of the locked oscillators. If $|w| > Kr^\alpha$, then we have

$$f(\theta, w) = \frac{C(w)g(w)}{w - Kr^\alpha \sin\theta}. \tag{14}$$

From the normalization condition in Eq. (6), $C(w)$ satisfies

$$C^{-1}(w) = \int_0^{2\pi} \frac{d\theta}{w - Kr^\alpha \sin\theta}, \tag{15}$$

which can be calculated to obtain

$$C(w) = \mathrm{sgn}(w)\frac{\sqrt{w^2 - (Kr^\alpha)^2}}{2\pi}, \tag{16}$$

with $\mathrm{sgn}(w)$ denoting the sign function of w. Obviously, $C(w)$ is an odd function of w. After inserting the above $C(w)$ back to Eq. (14), we arrive at the second expression in Eq. (11) for the density of the drifting oscillators.

C. Self-consistency equation for *r*

Next we will deduce the self-consistency equation of $r > 0$ for the partially locked states. In terms of the real and imaginary parts, Eq. (8) breaks up to

$$r\sin\psi = \int_{-\infty}^{+\infty}\int_0^{2\pi} \sin\theta f(\theta, w, t)d\theta dw \tag{17}$$

and

$$r\cos\psi = \int_{-\infty}^{+\infty}\int_0^{2\pi} \cos\theta f(\theta, w, t)d\theta dw. \tag{18}$$

The above two integrals in Eqs. (17) and (18) can be split into two parts according to whether $|w| \leqslant Kr^\alpha$ or $|w| > Kr^\alpha$, which correspond to the locked and drifting oscillators, respectively.

The integral in Eq. (17) for $|w| \leqslant Kr^\alpha$ is evaluated as

$$\begin{aligned} &\int_{|w|\leqslant Kr^\alpha}\int_0^{2\pi} \sin\theta f(\theta, w, t)d\theta dw \\ &= \int_{|w|\leqslant Kr^\alpha}\int_0^{2\pi} \sin\theta\delta\left(\theta - \arcsin(\frac{w}{Kr^\alpha})\right)g(w)d\theta dw \\ &= \int_{|w|\leqslant Kr^\alpha} \frac{w}{Kr^\alpha}g(w)dw \\ &= 0, \end{aligned} \tag{19}$$

and the part for $|w| > Kr^\alpha$ becomes

$$\begin{aligned} &\int_{|w|>Kr^\alpha}\int_0^{2\pi} \sin\theta f(\theta, w, t)d\theta dw \\ &= \int_{|w|>Kr^\alpha}\int_0^{2\pi} \sin\theta \frac{C(w)}{w - Kr^\alpha\sin\theta}g(w)d\theta dw \\ &= \int_{|w|>Kr^\alpha} \frac{wC(w)g(w)}{Kr^\alpha}\int_0^{2\pi}\left[\frac{1}{w - Kr^\alpha\sin\theta} - \frac{1}{w}\right]d\theta dw \\ &= \int_{|w|>Kr^\alpha} \frac{wC(w)g(w)}{Kr^\alpha}\left[\frac{1}{C(w)} - \frac{2\pi}{w}\right]dw \\ &= \int_{|w|>Kr^\alpha} \frac{[w - 2\pi C(w)]g(w)}{Kr^\alpha}dw \\ &= 0, \end{aligned} \tag{20}$$

because the integrand is an odd function of w. From Eqs. (19) and (20), we have $r\sin\psi = 0$, which is in accordance with the previous assumption of $\psi = 0$.

However, the integral in Eq. (18) for $|w| > Kr^\alpha$ can be calculated as

$$\begin{aligned} &\int_{|w|>Kr^\alpha}\int_0^{2\pi} \cos\theta f(\theta, w, t)d\theta dw \\ &= \int_{|w|>Kr^\alpha}\int_0^{2\pi} \frac{C(w)g(w)\cos\theta}{w - Kr^\alpha\sin\theta}d\theta dw \\ &= 0, \end{aligned} \tag{21}$$

since the integrand has a periodic antiderivative with the period of 2π. So, r is solely decided by Eq. (18) with $|w| \leqslant Kr^\alpha$, i.e.,

$$\begin{aligned} r &= \int_{-Kr^\alpha}^{Kr^\alpha}\int_0^{2\pi} \cos\theta f(\theta, w, t)d\theta dw \\ &= \int_{-Kr^\alpha}^{Kr^\alpha}\int_0^{2\pi} \cos\theta\delta\left(\theta - \arcsin(\frac{w}{Kr^\alpha})\right)g(w)d\theta dw \\ &= \int_{-Kr^\alpha}^{Kr^\alpha}\sqrt{1 - \left(\frac{w}{Kr^\alpha}\right)^2}\,g(w)dw, \end{aligned} \tag{22}$$

or equivalently

$$r = \int_{-1}^{1} \sqrt{1-s^2} g(Kr^{\alpha}s) Kr^{\alpha} ds, \tag{23}$$

which gives a complete description of the order parameter r of the steady states for Eq. (5)

The self-consistency Eq. (23) always has a trivial solution $r = 0$, which corresponds to the incoherent state with $f(\theta, w) = g(w)/2\pi$. Other branches of solution in Eq. (23) with $r \neq 0$, corresponding to the partially (or fully) locked states, obey

$$\frac{1}{Kr^{\alpha-1}} = \int_{-1}^{1} \sqrt{1-s^2} g(Kr^{\alpha}s) ds. \tag{24}$$

Let $p = Kr^{\alpha}$ and define a function $\Phi(p)$ as

$$\Phi(p) = \int_{-1}^{1} \sqrt{1-s^2} g(ps) ds, \tag{25}$$

all solutions of K and r for Eq. (24) can be parametrized by p as

$$K = p^{1-\alpha}\Phi^{-\alpha}(p) \quad \text{and} \quad r = p\Phi(p) \tag{26}$$

for $p \in (0, \infty)$, where $\Phi(p)$ is continuous, positive, and nonincreasing on $[0, \infty)$, and r is a monotonic increasing function of p. As

$$\lim_{p\to 0^+} \Phi(p) = \frac{\pi g(0)}{2}, \tag{27}$$

thus $r \to 0^+$ when $p \to 0^+$, then we have a critical coupling strength

$$K_c = \lim_{p\to 0^+} p^{1-\alpha}\Phi^{-\alpha}(p) = \begin{cases} 0 & \text{if } \alpha < 1 \\ \frac{2}{\pi g(0)} & \text{if } \alpha = 1 \\ +\infty & \text{if } \alpha > 1, \end{cases} \tag{28}$$

which gives the coupling threshold for the initial onset of partial locking.

With increasing p just beyond 0^+, the first oscillators with $|w| \leqslant Kr^{\alpha}$ start to phase-lock. For a larger value of p ($p = Kr^{\alpha}$), more oscillators are recruited into the synchronized pack. As further increasing p, the locked process persists forever if the support of $g(w)$ (defined as a set of w with $g(w) \neq 0$) is infinite, which implies that only the partially locked states are permissible. However, for other frequency distributions of $g(w)$ supported on a finite interval, e.g., $[-1, 1]$ without lack of generality, the process of phase locking starts at $p \to 0^+$, and is complete for $p = 1$. Thus, there has a second critical coupling strength

$$K_l = \Phi^{-\alpha}(1), \tag{29}$$

satisfying $Kr^{\alpha} = 1$; the partially locked states exist only if $0^+ < p < 1$, for $p \geqslant 1$ all the oscillators are entrained to the same common frequency, i.e., the fully locked state appears.

For a fixed value of α, the synchronization diagrams of r versus K for a given frequency distribution $g(w)$ can be detected from the two parametric equations in Eq. (26). However, the stability of the corresponding steady solutions of Eq. (5) is still elusive until here, which will be particularly

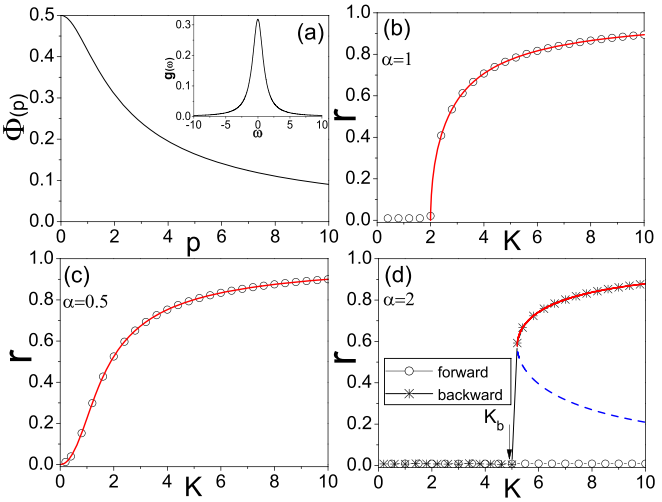

FIG. 1. (a) The plot of $\Phi(p)$ as a function of p in Eq. (30) for Lorentzian frequency distribution $g(w) = \Delta/\pi(w^2 + \Delta^2)$ with $\Delta = 1$. The upper-right inset shows the plot of $g(w)$. (b, c) Synchronization diagrams by plotting r as a function of K for $\alpha = 1$, 0.5, and 2, respectively. The theoretical prediction of r vs. K from Eq. (26) is depicted by the solid red line and the dashed blue line, which denote the stable partially locked states and the unstable ones, respectively. The open circles in (b) and (c) represent numerical results for the coupled system Eq. (3) with $N = 10\,000$ and random initial conditions, whereas the forward and backward continuations are adopted to numerically monitor the value of r as adiabatically increasing or decreasing K for $\alpha = 2$ in (d), marked by the black lines with open circles and stars, respectively. In the numerical simulations, the oscillators' natural frequencies are assigned as $w_j = \Delta \tan[(\pi/2)(2j - N - 1)/(N + 1)]$ [59].

treated in Sec. III. Figures 1, 2, and 3 show bifurcation diagrams of r versus K obtained from Eq. (26) for $g(w)$ to be Lorentzian, uniform, and triangle frequency distributions, respectively. The steady solutions of $r \neq 0$ from Eq. (26) are plotted by the red solid lines and the blue dashed lines, which correspond to the stable and unstable steady states, respectively. All the theoretical predictions of r on the stable branch are well confirmed by the results from the numerical simulations by directly integrating the coupled system Eq. (3) with $N = 10\,000$, where the natural frequencies w_j are sampled in a deterministic way for each of the distributions as in [59]. For $\alpha \leqslant 1$, random initial conditions are used, whereas for $\alpha > 1$, we adopt both forward and backward continuations to monitor the value of r as adiabatically increasing or decreasing K, which are indicated by the black lines with open circles and stars, respectively. In the following, we will present the detailed results for Lorentzian, uniform, and triangle frequency distributions, respectively.

1. Lorentzian frequency distribution

The Lorentzian distribution has the density function as

$$g(w) = \frac{\Delta}{\pi(w^2 + \Delta^2)},$$

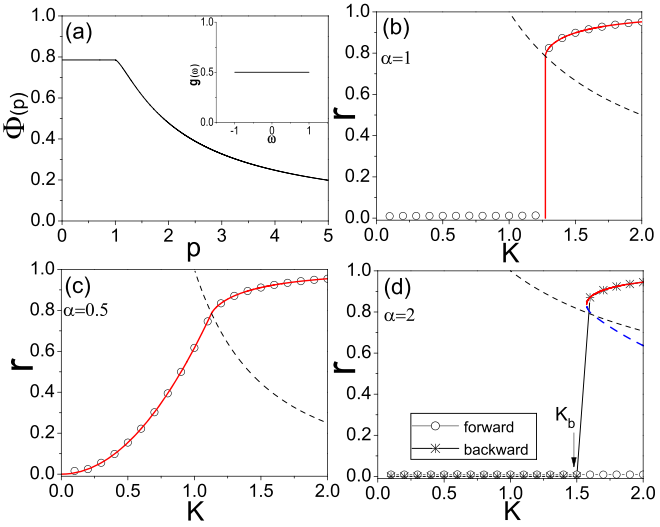

FIG. 2. The same as Fig. 1 for uniform frequency distribution prescribed by $g(w) = 1/2$ for $|w| \leqslant 1$, and 0 otherwise. The dashed black lines in the panels of (b–d) denote the hyperbola $Kr^{\alpha} = 1$. The points of (K, r) from Eq. (26) below and above the hyperbola $Kr^{\alpha} = 1$ correspond to the partially locked states and the fully locked ones, respectively. The solid red lines in (b–d) mark the stable steady states, whereas the dashed blue line in (d) represents the unstable steady states. In the numerical simulations, the oscillators' natural frequencies are assigned as $w_j = (2j - N - 1)/(N - 1)$ [59].

where $\Delta = 1$ is fixed in the numerical simulations. Equation (25) can then be integrated to yield

$$\Phi(p) = \frac{1}{\Delta + \sqrt{\Delta^2 + p^2}},$$

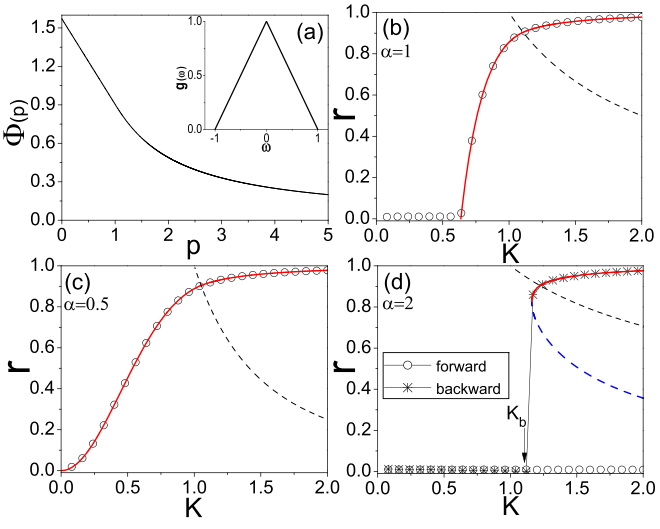

FIG. 3. The same as described in the caption of Fig. 2 for triangle frequency distribution prescribed by $g(w) = 1 - |w|$ for $|w| < 1$, and 0 otherwise. In the numerical simulations, the oscillators' natural frequencies are assigned as $w_j = \sqrt{2(j-1)/(N-1)} - 1$ for $j < (N+1)/2$ and $w_j = 1 - \sqrt{2(N-j)/(N-1)}$ for $j > (N+1)/2$ [59].

which is plotted in Fig. 1(a) with $g(w)$ shown in the upper-right corner. As Lorentzian frequency distribution has infinite support $(-\infty, +\infty)$, the full locking is never achieved for any $K > 0$. For $\alpha = 1$, a second-order phase transition to partial locking has been well established, i.e., the partially locked state bifurcates continuously from the incoherent state $r = 0$ at $K_c = 2\Delta$, which is reproduced in Fig. 1(b). Synchronization diagrams of r versus K for $\alpha \neq 1$ are distinctly different from that of $\alpha = 1$. For $\alpha = 0.5$ in Fig. 1(c), we find that the partially locked state emerges continuously from $r = 0$ at $K_c = 0$ and is stable for all $K > 0$, whereas the incoherent is unstable for any $K > 0$. Interestingly, for $\alpha = 2$ in Fig. 1(d), the incoherent state is numerically observed to be linearly stable for all $K > 0$, whereas the partial locking is initiated at $K = K_c \to \infty$. One branch of the partially locked states is stabilized with pronounced values of $r > 0$ if K is beyond a certain coupling threshold K_b, which is always accompanied by the other unstable branch. For $K > K_b$, there exists a bistability between the partially locked states and the incoherent state. Thus, at $K = K_b$, the transition to synchronization may occur in an abrupt way manifested via a jump of r from zero to a pronounced positive value in numerical simulations with special initial conditions, which mimics a first-order transition at the onset of synchronization but in the absence of hysteretic behavior. In fact, as adiabatically decreasing K from a sufficiently large value, an abrupt desynchronization transition appears at $K = K_b$, whereas there is no counterpart of abrupt synchronization transition as adiabatically increasing K from zero, which has been exclusively reported in globally coupled oscillator simplexes quite recently [60–62].

2. *Uniform frequency distribution*

Let

$$g(w) = \begin{cases} \frac{1}{2} & \text{if } |w| \leqslant 1 \\ 0 & \text{if } |w| > 1, \end{cases}$$

which corresponds to a uniform distribution of frequencies over the interval of $[-1, 1]$. Equation (25) then becomes

$$\Phi(p) = \begin{cases} \frac{\pi}{4} & \text{if } 0 < p \leqslant 1 \\ \frac{1}{2}\left(\arcsin\frac{1}{p} + \frac{\sqrt{p^2-1}}{p^2}\right) & \text{if } p > 1. \end{cases}$$

Figure 2(a) plots the function of $\Phi(p)$ calculated from the uniform frequency distribution $g(w)$ shown in the upper-right corner. Now $g(w)$ has a finite (compact) support of $[-1, 1]$, the onset of partial locking starts at $p \to 0^+$ and ends up at $p = 1$, which correspond to two critical coupling strengths K_c and K_l given by Eqs. (28) and (29), respectively. The points (K, r) from Eq. (26) that are below and above the hyperbola of $Kr^{\alpha} = 1$ (i.e., $p = 1$), plotted by the black dashed lines in Figs. 2(b)–2(d), correspond to the partially and fully locked states, respectively. For $\alpha = 1$, the partial locking is onset and complete at the same coupling strength $K = K_c = K_l = 4/\pi$, at which r continuously and monotonically increases from $r = 0$ to $r = \pi/4$ as increasing p from $p \to 0^+$ to $p = 1$. Thus, synchronization diagram for $\alpha = 1$ in Fig. 2(b) has a vertical segment at $K = 4/\pi$, corresponding to infinitely many partially locked states with $0 < r < 4/\pi$; full locking is achieved for $K > 4/\pi$. Note that r jumps from zero to a finite value of $r = \pi/4$ for an infinitesimal variation of the

coupling strength K around $K_c = 4/\pi$, i.e., $\lim_{K\to K_c^-} r = 0 \neq \lim_{K\to K_c^+} r = \pi/4$. The phase transition to synchronization for the uniform distribution of the natural frequencies shown in Fig. 2(b) for $\alpha = 1$ is of first-order type [63], which can be extended to frequency distributions $g(w)$ with a plateau at their maximum [64]. For $\alpha = 0.5$ in Fig. 2(c), one can clearly observe that the partial locking begins at $K = K_c = 0$, and is complete at $K_l = \Phi^{-\alpha}(1) = (\pi/4)^{-0.5} \approx 1.13$, then the full locking is established for all $K \geqslant K_l \approx 1.13$. Interestingly, for $\alpha = 2$ in Fig. 2(d), we find that the partially locked states are always unstable as increasing p from 0^+ to 1, and the full locked state is not immediately stabilized when the partial locking is complete at $p = 1$, which becomes stabilized for p far beyond 1 with $K > K_b \approx 1.57$. With adiabatically decreasing K from $K > K_b$, an abrupt desynchronization is manifested via the transition from the fully locked state to the incoherent state at $K = K_b \approx 1.57$.

3. Triangle frequency distribution

In the following, we consider a triangle distribution of frequencies over $[-1, 1]$:

$$g(w) = \begin{cases} 1 - |w| & \text{if } |w| \leqslant 1 \\ 0 & \text{if } |w| > 1, \end{cases}$$

which is provided to make a comparison with the case of the uniform frequency distribution. Substitution of the above $g(w)$ into Eq. (25) yields

$$\Phi(p) = \begin{cases} \frac{\pi}{2} - \frac{2p}{3} & \text{if } 0 < p \leqslant 1 \\ \arcsin\frac{1}{p} + \frac{\sqrt{p^2-1}}{p^2} - \frac{2p}{3}\left[1 - \left(\frac{p^2-1}{p^2}\right)^{\frac{3}{2}}\right] & \text{if } p > 1. \end{cases}$$

Figure 3(a) portraits the function of $\Phi(p)$ with the corresponding $g(w)$ in the up-right inset, which has a finite (compact) support of $(-1, 1)$ implying the existence of two critical coupling strengths K_c and K_l. A typical second-order phase transition to partial locking is retrieved in Fig. 3(b) for $\alpha = 1$. As increasing K from zero, the onset of partial locking takes place at $K = K_c = 2/(\pi g(0)) \approx 0.64$, and is complete at another coupling value of $K_l = \Phi^{-\alpha}(1) = (\pi/2 - 2/3)^{-1} \approx 1.1$, which is different from the case of uniform frequency distribution with $K_c = K_l$ shown in Fig. 2(b). For $\alpha = 0.5$, the synchronization diagram in Fig. 3(c) is quite similar to that in Fig. 2(c), where the corresponding two critical coupling thresholds are now given by $K_c = 0$ and $K_l = \Phi^{-\alpha}(1) = (\pi/2 - 2/3)^{-0.5} \approx 1.05$, respectively. For $\alpha = 2$ in Fig. 3(d), one branch of the partially locked states is found to be stabilized at $K_b \approx 1.16$ with a finite value of $r > 0$, which remains stable for an interval of $[K_b, K_l)$ with $K_l = \Phi^{-\alpha}(1) = (\pi/2 - 2/3)^{-2} \approx 1.22$. A unique branch of the fully locked states emerges at $K = K_l \approx 1.22$ and is stable for all $K \geqslant K_l \approx 1.22$. When progressively decreasing K from a sufficiently large value, the partially locked state transits abruptly to the incoherent state at $K = K_b \approx 1.16$.

D. Average effective frequencies

The appearance of partially (fully) locked state can be directly clarified by calculating the average effective frequencies defined by

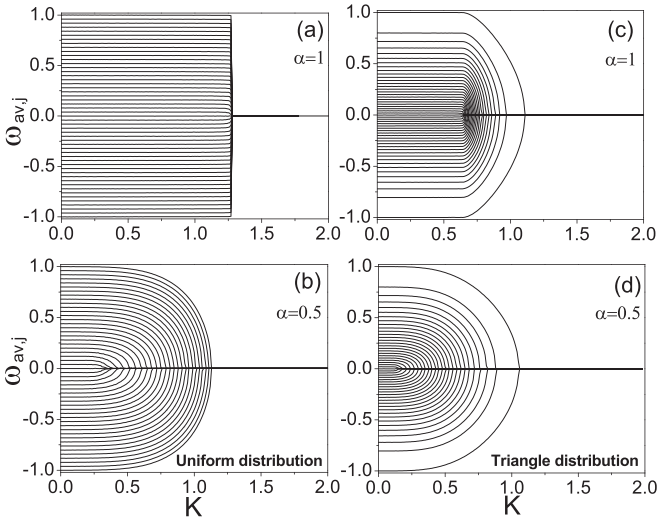

FIG. 4. (a, b) Bifurcation trees of the average effective frequency $w_{\mathrm{av},j}$ vs. the coupling strength K for $\alpha = 1$ and 0.5 with the natural frequencies uniformly distributed over $[-1, 1]$. (c, d) The same as (a) and (b) with the triangle distribution of frequencies over $[-1, 1]$ considered. The average effective frequencies $w_{\mathrm{av},j}$ are numerically calculated from the coupled system Eq. (3) with $N = 1000$. For clarity, the results for only a subset of the 50 oscillators are represented in each panel.

$$w_{\mathrm{av},j} := \lim_{\tau\to\infty} \int_0^\tau \dot{\theta}_j(t)dt = \lim_{\tau\to\infty} \frac{\theta_j(\tau) - \theta_j(0)}{\tau}. \quad (30)$$

In the thermodynamic limit, the time-averaged quantity in Eq. (30) can be analytically predicted by averaging the phase velocity $v(\theta, w, t)$ for $0 \leqslant \theta \leqslant 2\pi$ with a fixed value of w under the conditional probability $f(\theta, w, t)/g(w)$ as

$$\begin{aligned} w_{\mathrm{av}}(w) &= \int_0^{2\pi} v(\theta, w, t)\frac{f(\theta, w, t)}{g(w)}d\theta \\ &= \frac{1}{g(w)}\int_0^{2\pi} (w - Kr^\alpha \sin\theta) f_{\mathrm{PLS}}(\theta, w)d\theta \\ &= \begin{cases} 0 & \text{if } |w| \leqslant Kr^\alpha \\ \mathrm{sgn}(w)\sqrt{w^2 - (Kr^\alpha)^2} & \text{if } |w| > Kr^\alpha. \end{cases} \end{aligned} \quad (31)$$

Clearly, the average effective frequencies for the locked oscillators with $|w| \leqslant Kr^\alpha$ equal to zero, whereas the drifting oscillators with $|w| > Kr^\alpha$ have different average effective frequencies dependent on K, w, r, and α. For two extreme cases, all the oscillators have $w_{\mathrm{av}}(w) = w$ for the incoherent state, whereas $w_{\mathrm{av}}(w) = 0$ holds for the fully locked states.

In Fig. 4 we present bifurcation trees of $w_{\mathrm{av},j}$ versus K, where $g(w)$ is adopted to be the uniform distribution in Figs. 4(a) and 4(b) with $\alpha = 1$ and 0.5 and the triangle distribution for Figs. 4(c) and 4(d) with $\alpha = 1$ and 0.5, respectively. For each fixed K, the average effective frequencies $w_{\mathrm{av},j}$ are numerically computed by integrating the coupled system Eq. (3) with $N = 1000$ and random initial conditions. Figure 4 gives a complementary view of synchronization diagrams of r versus K for the coupled system Eq. (3), which clearly reveals three distinctive routes to synchronization with increasing K

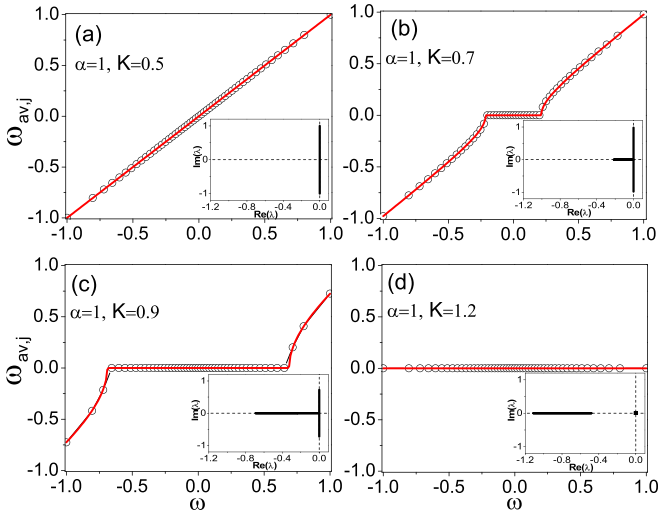

FIG. 5. The average effective frequency $w_{\mathrm{av,j}}$ vs. the natural frequency w for (a) the incoherent state with $K = 0.5$, (b, c) the partially locked states with $K = 0.7$ and $K = 0.9$, and (d) the fully locked state with $K = 1.2$, respectively. $g(w)$ is taken to be the triangle distribution and $\alpha = 1$ is fixed. In all panels, the open circles denote the numerical data directly extracted from Fig. 4(c), which agrees well with the analytical prediction w_{av} in Eq. (31) plotted by the red lines. The lower-right inset in each subfigure shows the spectrum for the corresponding steady state in the thermodynamic limit $N \to \infty$.

from zero. From Fig. 4(a), it is observed that the system undergoes an abrupt transitions from a totally incoherent state to a fully locked state at $K = 4/\pi$, which is due to the process of partial locking is initiated and complete at a single coupling strength $K = K_c = K_l = 4/\pi$ for the uniform distribution $g(w)$ and $\alpha = 1$. The bifurcation trees in Figs. 4(b) and 4(d) show that the partial locking takes place at $K = K_c = 0$ for $\alpha < 1$, which is independent of the frequency distribution $g(w)$. As gradually increasing K from zero, it can be observed that the oscillators with the natural frequencies close to zero are successively entrained to the center, and the synchronized cluster grows until all the drifting oscillators are absorbed at $K = K_l > 0$, after that the fully locked states are established for $K > K_l$. Figure 4(c) corroborates that the coupled systems Eq. (3) with $\alpha = 1$ experiences a transition from the totally incoherent state to the partially locked state at $K = K_c > 0$, and then the fully locked state is achieved for $K = K_l > K_c$, which is in congruence with the synchronization diagram in Fig. 3(b).

Figure 5 further depicts the dependence of the average effective frequency $w_{\mathrm{av,j}}$ on the natural frequency w for various steady states with different coupling values of K, where $\alpha = 1$ is fixed and $g(w)$ is prescribed by the triangle distribution. Clearly, as gradually increasing the coupling strength K, the coupled system experiences from the incoherent state [Fig. 5(a) with $K = 0.5$], via the partially locked states [Figs. 5(b) and 5(c) with $K = 0.7$ and 0.9], to the fully locked state [Fig. 5(d) with $K = 1.2$], respectively. In all the panels of Figs. 5(a)–5(d), the open circles mark the numerical data, extracted correspondingly from Fig. 4(c), which are well predicted by $w_{\mathrm{av}}(w)$ in Eq. (31) indicated by the red lines. Moreover, in the lower-right inset of each subfigure, we portray the spectrum for the corresponding steady state, which will be analytically derived in the thermodynamic limit of $N \to \infty$ in Sec. III. We would like to stress that the validity of $w_{\mathrm{av}}(w)$ in Eq. (31) has been corroborated for other values of $\alpha \neq 1$ and the different types of frequency distribution $g(w)$, where a similar agreement between the numerical simulations and the theoretical results has been observed as in Fig. 5.

III. STABILITY ANALYSIS OF STEADY SOLUTIONS

The above section reveals that the structures of steady states for the system can be thoroughly explored through the self-consistency equation in the frame of mean-field theory, which, however, cannot address the stability of corresponding steady states. In this section, we will analyze the linear stability of the incoherent state and of the partially (fully) locked states of coupled system Eq. (3) in the thermodynamic limit $N \to \infty$. For the limit of large N, the macroscopic dynamics of coupled system Eq. (3) can be well characterized by the density function $f(\theta, w, t)$ governed by Eq. (5), which is a nonlinear partial differential equation. In the following, we will show that the spectrum of both the incoherent state and the partially (fully) locked states can be systematically worked out from a frequency dependent version of the Ott-Antonsen system represented by a nonlinear ordinary integrodifferential equation.

A. The Ott-Antonsen approach

Since the density function $f(\theta, w, t)$ is required to be 2π-periodic in θ, we can expand in the form of the Fourier series

$$f(\theta, w, t) = \frac{1}{2\pi} \sum_{n=-\infty}^{+\infty} z_n(t, w) e^{-in\theta}, \tag{32}$$

with the nth Fourier coefficient

$$z_n(t, w) = \int_0^{2\pi} e^{in\theta} f(\theta, w, t) d\theta, \quad n = 0, 1, 2, \ldots, \tag{33}$$

where $z_0(t, w) = g(w)$ and $z_{-n}(t, w) = z_n^*(t, w)$. $z_n^*(t, w)$ denotes the complex conjugate of $z_n(t, w)$. From the continuity Eq. (5) and the velocity in Eq. (7), we can get that the evolutions of $z_n(t, w)$ are determined by the differential equations

$$\frac{\partial z_n}{\partial t} = niwz_n + \frac{nK}{2}[H(t)z_{n-1} - H^*(t)z_{n+1}], \tag{34}$$

with $n \geqslant 1$.

By adopting the Ott-Antonsen *ansatz*, i.e., $z_n(t, w) = z^n(t, w)g(w)$ [26,27], Eq. (34) is reduced to

$$\frac{\partial z(t, w)}{\partial t} = iwz(t, w) + \frac{K}{2}H(t) - \frac{K}{2}H^*(t)z^2(t, w), \tag{35}$$

with $H(t) = r^\alpha e^{i\psi}$ as in Eq. (7). The amplitude $r(t)$ and phase $\psi(t)$ of the order parameter are now given by

$$R = re^{i\psi} = \int_{-\infty}^{+\infty} z(t, w)g(w)dw := \widehat{P}z(t, w), \tag{36}$$

where $\widehat{P}$ denotes the integral operator defined as above. Equations (35) and (36) with $|z(t, w)| \leqslant 1$ constitute as a closed reduced Ott-Antonsen system, which is invariant with respect

to the phase shift $z(t,w) \to z(t,w)e^{i\phi}$. The spectral analysis of both the incoherent state and the partially (fully) locked states will be conducted from Eqs. (35) and (36) within a unified framework based on spectral theory of linear operators [65]. Before that, we need to identify the solutions of $z(t,w)$ for the incoherent and the partially locked states, respectively.

By performing the summation of series in Eq. (32) for $|z(t,w)| \leqslant 1$, we obtain

$$f(\theta,w,t) = \frac{g(w)}{2\pi}\frac{(1-|z|)(1+|z|)}{(1-|z|)^2+4|z|\sin^2(\frac{\theta-\arg z}{2})}. \quad (37)$$

Clearly, from Eq. (37), we have $f(\theta,w,t) = g(w)/(2\pi)$ if $z(t,w)=0$, which is a trivial solution of Eq. (35) with $r=0$ corresponding to the incoherent state. However, for $z(t,w)\neq 0$, the density degenerates to $f(\theta,w,t)=\delta(\theta-\arg z)g(w)$ if $|z(t,w)|=1$, whereas $f(\theta,w,t)$ is a unimodal distribution in the phase θ with the center located on $\arg z$ for any w at time t if $|z(t,w)|<1$. The locked and drifting oscillators in the partially locked states are perfectly characterized by $|z(t,w)|=1$ and $|z(t,w)|<1$, respectively.

To derive $z(t,w)$ for the partially locked states, we look for the nonzero steady solution of system Eq. (35) in the form of $z(t,w)=\beta(s)$, where $\beta(s)$ is decided by

$$\beta^2(s) - 2is\beta(s) - 1 = 0, \quad (38)$$

with $s = w/Kr^\alpha$. It is easy to get one root from Eq. (38) as

$$\beta(s) = \begin{cases} is+\sqrt{1-s^2} & \text{if } s\leqslant 1 \\ is(1-\sqrt{1-s^{-2}}) & \text{if } s>1, \end{cases} \quad (39)$$

where $|\beta(s)|=1$ holds for $|s|\leqslant 1$ and $|\beta(s)|<1$ for $|s|>1$. The root $\beta(s)$ in Eq. (39) with $s=w/Kr^\alpha$ gives the steady solution of $z(t,w)$ in Eq. (35) for the partially locked states, which can be verified in a self-consistency way provided in Appendix A. Moreover, we have

$$\begin{aligned} r &= \int_{-\infty}^{+\infty} z(t,w)g(w)dw = \int_{-\infty}^{+\infty}\beta\left(\frac{w}{Kr^\alpha}\right)g(w)dw \\ &= \int_{-\infty}^{+\infty}\beta(s)g(Kr^\alpha s)Kr^\alpha ds \\ &= \int_{-1}^{1}\sqrt{1-s^2}g(Kr^\alpha s)Kr^\alpha ds, \end{aligned}$$

which recreates the self-consistency equation for r as the same in Eq. (23), thus further confirming the steady solution of $z(t,w)$ in Eq. (39) for the partially locked states.

B. Stability of incoherent state

We begin to analyze the linear stability of the incoherent state by introducing a small perturbation away from the trivial solution $z(t,w)=0$:

$$z(t,w) = 0 + \varepsilon v(t,w), \quad (40)$$

where $\varepsilon \ll 1$. After incorporating the perturbation Eq. (40), $H(t)$ in the right-hand side of Eq. (35) becomes

$$\begin{aligned} H(t) &= R^{\frac{\alpha+1}{2}}R^{*\frac{\alpha-1}{2}} \\ &= (\varepsilon\widehat{P}v)^{\frac{\alpha+1}{2}}(\varepsilon\widehat{P}v^*)^{\frac{\alpha-1}{2}} \\ &= \varepsilon^\alpha(\widehat{P}v)^{\frac{\alpha+1}{2}}(\widehat{P}v^*)^{\frac{\alpha-1}{2}}. \end{aligned} \quad (41)$$

Then, by substituting Eqs. (40) and (41) into Eq. (35), the evolution of the perturbation is given by

$$\frac{\partial v}{\partial t} = iwv + \frac{K}{2}\varepsilon^{\alpha-1}(\widehat{P}v^*)^{\frac{\alpha-1}{2}}(\widehat{P}v)^{\frac{\alpha+1}{2}} + o(\varepsilon). \quad (42)$$

It can be seen that if $\alpha<1$, the second term in the right-hand side of Eq. (42) goes to infinite as $\varepsilon\to 0$, which implies that the linear perturbation v in Eq. (42) diverges with time. Thus, we conclude that the incoherent state is unstable for any $K>0$ when $\alpha<1$.

In contrast, if $\alpha>1$, then the second term associated with the coupling strength K in the right-hand side of Eq. (42) will be absorbed to $o(\varepsilon)$, in which case only the first one survives at $o(\varepsilon)$. The coupling between the oscillators makes no contribution to the evolution of the linear perturbation. Therefore, one can infer that the perturbation v does not grow nor decay with time, which means that the incoherent state keeps always linearly neutrally stable for $K>0$ if $\alpha>1$.

For $\alpha=1$, the evolution Eq. (42) at $o(\varepsilon)$ becomes

$$\frac{\partial v}{\partial t} = iwv + \frac{K}{2}\widehat{P}v. \quad (43)$$

Since the perturbation v in Eq. (43) is complex-valued, its complex conjugated term v^* should be considered for completeness. Introducing the vector-function as

$$\overrightarrow{V(t)} = \begin{pmatrix} v(t,w) \\ v^*(t,w) \end{pmatrix},$$

we have

$$\frac{\partial\overrightarrow{V}}{\partial t} = L\overrightarrow{V} \quad \text{with} \quad L = L_1 + L_2,$$

where L_1 is a multiplication operator defined by

$$L_1\overrightarrow{V} = \begin{pmatrix} iw & 0 \\ 0 & -iw \end{pmatrix}\begin{pmatrix} v \\ v^* \end{pmatrix},$$

and L_2 is an integral operator given by

$$L_2\overrightarrow{V} = \frac{K}{2}\widehat{P}\overrightarrow{V} = \frac{K}{2}\int_{-\infty}^{+\infty} g(w)\overrightarrow{V}\,dw.$$

The operator L_1 is completely uncoupled in the sense that $L_1\overrightarrow{V}$ depends only on w, whereas the coupling of the oscillators is only involved in the operator L_2.

The linear operator L has both a continuous and a discrete spectrum [65]. The continuous spectrum of the linear operator L consists of λ by solving equation

$$\det(\lambda I - L_1) = \det\begin{pmatrix} \lambda - iw & 0 \\ 0 & \lambda + iw \end{pmatrix} = 0,$$

from which one can easily calculate

$$\sigma_{cs}(L) = \{\lambda = iw : w \in \text{Support}(g)\}.$$

The above formula indicates that the continuous spectrum $\sigma_{cs}(L)$ lies exactly on the imaginary axis, which is always neutral and cannot induce a linear instability of the incoherent state.

The discrete spectrum of the linear operator L is obtained by seeking nontrivial solutions of the equation

$$L\overrightarrow{V} = \lambda\overrightarrow{V}. \tag{44}$$

Substituting the explicit forms of the operators L_1 and L_2, we can transform Eq. (44) into

$$\overrightarrow{V} = \frac{K}{2}(\lambda I - L_1)^{-1}\widehat{P}\overrightarrow{V}, \tag{45}$$

where $\lambda I - L_1$ is invertible for $\lambda \notin \sigma_{cs}(L)$. Applying the integral operator $\widehat{P}$ to both sides of Eq. (45), we arrive at

$$\left[I - \frac{K}{2}\widehat{P}(\lambda I - L_1)^{-1}\right]\widehat{P}\overrightarrow{V} = 0,$$

which yields the characteristic equation for the discrete spectrum of linear operator L as

$$\det\left[I - \frac{K}{2}\widehat{P}(\lambda I - L_1)^{-1}\right] = 0, \tag{46}$$

with

$$(\lambda I - L_1)^{-1} = \begin{pmatrix} \frac{1}{\lambda - iw} & 0 \\ 0 & \frac{1}{\lambda + iw} \end{pmatrix}.$$

After straightforward calculations, Eq. (46) becomes equivalent to

$$1 - \frac{K}{2}\int_{-\infty}^{+\infty}\frac{\lambda g(w)}{\lambda^2 + w^2}dw = 0, \tag{47}$$

which has only the possibility of positive real roots for symmetric and unimodal distributions $g(w)$. By letting $\lambda \to 0^+$ in Eq. (47), one obtains

$$K_c = \frac{2}{\pi g(0)},$$

above which the discrete spectrum appears in the right half-plane $\mathrm{Re}\lambda > 0$, implying the instability of incoherent state. Thus, the incoherent state is linearly neutrally stable for $K < K_c = \frac{2}{\pi g(0)}$ and unstable for $K > K_c = \frac{2}{\pi g(0)}$, which exactly recovers the well-known result for the standard Kuramoto model.

As mentioned in the Introduction, in the case of $\alpha = 1$ for the classic Kuramoto model, the first rigorous stability analysis of the incoherent state has been well made by Strogatz and Mirollo in Ref. [18], where they carried out their study by directly linearizing the continuity equation (5) about the incoherent state $f = g(w)/(2\pi)$. Here, we have illustrated that all the information about linear stability of incoherent state for the Kuramoto model can be successfully retrieved from the reduced Ott-Antonsen system of Eqs. (35) and (36) with $\alpha = 1$.

C. Stability of partially locked states

In this subsection, we turn our attention to the stability analysis of partially locked states, which can be carried out in a similar way as that for the incoherent state presented in Sec. III B. Let us consider a small perturbation away from the steady solution in Eq. (39):

$$z(t, w) = \beta(w/Kr^\alpha) + \varepsilon v(t, w), \tag{48}$$

with $\varepsilon \ll 1$. The perturbed $H(t)$ is evaluated as

$$\begin{aligned} H(t) &= R^{\frac{\alpha+1}{2}}R^{*\frac{\alpha-1}{2}} \\ &= (r + \varepsilon\widehat{P}v)^{\frac{\alpha+1}{2}}(r + \varepsilon\widehat{P}v^*)^{\frac{\alpha-1}{2}} \\ &= r^\alpha + \varepsilon r^{\alpha-1}\left[\frac{\alpha+1}{2}\widehat{P}v + \frac{\alpha-1}{2}\widehat{P}v^*\right] + o(\varepsilon^2). \end{aligned}$$

To linearize Eq. (35), insert $z(t, w) = \beta(w/Kr^\alpha) + \varepsilon v(t, w)$ and the above perturbed $H(t)$, after gathering all the linear terms in the first order of ε, we obtain the evolution of the perturbation $v(t, w)$ governed by the equation

$$\frac{\partial v}{\partial t} = \eta(w)v + \frac{K}{4}r^{\alpha-1}(\mu\widehat{P}v + \nu\widehat{P}v^*), \tag{49}$$

where $\eta(w) = iw - Kr^\alpha\beta(w/Kr^\alpha)$, $\mu = (\alpha+1) - (\alpha-1)\beta^2(w/Kr^\alpha)$, and $\nu = (\alpha-1) - (\alpha+1)\beta^2(w/Kr^\alpha)$. As before, we need to switch to the vector-function $\overrightarrow{V} = \binom{v}{v^*}$, which has again the form of

$$\frac{\partial\overrightarrow{V}}{\partial t} = L\overrightarrow{V} \quad \text{with} \quad L = L_1 + L_2,$$

where the multiplication operator L_1 is now given by

$$L_1\overrightarrow{V} = \begin{pmatrix} \eta(w) & 0 \\ 0 & \eta^*(w) \end{pmatrix}\begin{pmatrix} v \\ v^* \end{pmatrix}, \tag{50}$$

and the integral operator L_2 by

$$L_2\overrightarrow{V} = \frac{K}{4}r^{\alpha-1}Q\widehat{P}\overrightarrow{V} = \frac{K}{4}r^{\alpha-1}Q\int_{-\infty}^{+\infty}g(w)\overrightarrow{V}\,dw, \tag{51}$$

with

$$Q = \begin{pmatrix} \mu & \nu \\ \nu^* & \mu^* \end{pmatrix}. \tag{52}$$

Again, the continuous spectrum $\sigma_{cs}(L)$ of the linear operator L is given by solving equation

$$\det(\lambda I - L_1) = \det\begin{pmatrix} \lambda - \eta(w) & 0 \\ 0 & \lambda - \eta^*(w) \end{pmatrix} = 0,$$

which implies

$$\sigma_{cs}(L) = \{\lambda = \eta(w), \eta^*(w) : w \in \mathrm{Support}(g)\},$$

with

$$\begin{aligned} \eta(w) &= iw - kr^\alpha\beta\left(\frac{w}{Kr^\alpha}\right) \\ &= \begin{cases} -\sqrt{(Kr^\alpha)^2 - w^2} & \text{if } |w| \leqslant Kr^\alpha \\ iw\sqrt{1 - \left(\frac{Kr^\alpha}{w}\right)^2} & \text{if } |w| > Kr^\alpha. \end{cases} \end{aligned}$$

Obviously, the partially locked states have a T-shaped continuous spectrum $\sigma_{cs}(L)$ in the complex plane, where a symmetric interval along the imaginary axis is generated by the drifting oscillators with $|w| > Kr^\alpha$, and another interval on the negative side of the real axis arises due to the locked oscillators with $|w| \leqslant Kr^\alpha$. Hence, similar to the incoherent

state, the continuous spectrum of the partially locked states is always neutral, where the instability is only possible to be caused by discrete spectrum. In contrast, the fully locked states, which require $|w| \leqslant Kr^{\alpha}$ for all $w \in \text{Support}(g)$, are always linearly stable with respective to their continuous spectrum.

The discrete spectrum of the linear operator L consists of $\lambda \notin \sigma_{\text{cs}}(L)$ for the equation

$$L\overrightarrow{V} = \lambda\overrightarrow{V}$$

having a nontrivial solution $\overrightarrow{V}$. After some transformations, the above equation can be rewritten as

$$\overrightarrow{V} = \frac{K}{4}r^{\alpha-1}(\lambda I - L_1)^{-1}Q\widehat{P}\overrightarrow{V}. \tag{53}$$

Applying the operator $\widehat{P}$ to both sides of Eq. (53), we can get

$$\left[I - \frac{K}{4}r^{\alpha-1}\widehat{P}(\lambda I - L_1)^{-1}Q\right]\widehat{P}\overrightarrow{V} = 0,$$

which leads to the characteristic equation of discrete spectrum

$$\det\left(I - \frac{K}{4}r^{\alpha-1}\widehat{P}(\lambda I - L_1)^{-1}Q\right) = 0, \tag{54}$$

with

$$(\lambda I - L_1)^{-1} = \begin{pmatrix} \frac{1}{\lambda-\eta(w)} & 0 \\ 0 & \frac{1}{\lambda+\eta^*(w)} \end{pmatrix}.$$

The partially (fully) locked states are unstable if Eq. (54) has a root λ with positive real part.

To derive explicit equations for the discrete spectrum λ, we rewrite the characteristic Eq. (54) as

$$\det\left[I - \frac{K}{4}r^{\alpha-1}M(\lambda, r)\right] = 0,$$

with

$$M(\lambda, r) = \widehat{P}(\lambda I - L_1)^{-1}Q = \begin{pmatrix} J_1(\lambda, r) & J_2(\lambda, r) \\ J_2^*(\lambda^*, r) & J_1^*(\lambda^*, r) \end{pmatrix},$$

where

$$J_1(\lambda, r) = \widehat{P}\frac{(\alpha+1) - (\alpha-1)\beta^2(\frac{w}{Kr^{\alpha}})}{\lambda - \eta(w)} = \int_{-\infty}^{+\infty} \frac{(\alpha+1) - (\alpha-1)\beta^2\left(\frac{w}{Kr^{\alpha}}\right)}{\lambda - iw + Kr^{\alpha}\beta\left(\frac{w}{Kr^{\alpha}}\right)}g(w)dw$$

and

$$J_2(\lambda, r) = \widehat{P}\frac{(\alpha-1) - (\alpha+1)\beta^2\left(\frac{w}{Kr^{\alpha}}\right)}{\lambda - \eta(w)} = \int_{-\infty}^{+\infty} \frac{(\alpha-1) - (\alpha+1)\beta^2(\frac{w}{Kr^{\alpha}})}{\lambda - iw + Kr^{\alpha}\beta\left(\frac{w}{Kr^{\alpha}}\right)}g(w)dw.$$

It can be proved by straightforward calculations that

$$J_1(\lambda, r) = J_1^*(\lambda^*, r) \quad \text{and} \quad J_2(\lambda, r) = J_2^*(\lambda^*, r)$$

hold for symmetric and unimodal distribution $g(w)$. Thus, the characteristic Eq. (54) is reduced to

$$1 - \frac{K}{4}r^{\alpha-1}[J_1(\lambda, r) - J_2(\lambda, r)] = 0 \tag{55}$$

and

$$1 - \frac{K}{4}r^{\alpha-1}[J_1(\lambda, r) + J_2(\lambda, r)] = 0, \tag{56}$$

respectively. After lots of tedious computations, one obtains that Eq. (55) is equivalent to

$$h_s(\lambda) = \frac{1}{Kr^{\alpha-1}}, \tag{57}$$

with

$$h_s(\lambda) = \int_{|s|\leqslant 1} \frac{1-s^2}{\left(\frac{\lambda}{Kr^{\alpha}}\right) + \sqrt{1-s^2}}g(Kr^{\alpha}s)ds + \int_{|s|>1} \frac{\left(\frac{\lambda}{Kr^{\alpha}}\right)[1 - s^2(1 - \sqrt{1-s^{-2}})]}{\left(\frac{\lambda}{Kr^{\alpha}}\right)^2 + s^2 - 1}g(Kr^{\alpha}s)ds,$$

and Eq. (56) to

$$h_c(\lambda) = \frac{1}{\alpha Kr^{\alpha-1}}, \tag{58}$$

with

$$h_c(\lambda) = \int_{|s|\leqslant 1} \frac{s^2}{\left(\frac{\lambda}{Kr^{\alpha}}\right) + \sqrt{1-s^2}}g(Kr^{\alpha}s)ds + \int_{|s|>1} \frac{\left(\frac{\lambda}{Kr^{\alpha}}\right)s^2(1 - \sqrt{1-s^{-2}})}{\left(\frac{\lambda}{Kr^{\alpha}}\right)^2 + s^2 - 1}g(Kr^{\alpha}s)ds.$$

Equations (57) and (58) completely describe the discrete spectrum of partially locked states. For the fully locked states, as $|w| \leqslant Kr^{\alpha}$ (i.e., $|s| < 1$) is satisfied for all the oscillators, the discrete spectrum of fully locked states is decided by Eqs. (57) and (58) involving only the first integral with $|s| \leqslant 1$.

From the self-consistency equation of r in Eq. (24), one can see that Eq. (57) always holds for $\lambda = 0$, i.e., the characteristic equation (54) has a root of $\lambda = 0$ irrespective of the values of parameters K, r, and α. The discrete spectrum must contain $\lambda = 0$, which is a consequence of the rotational symmetry of the original phase-model in Eq. (3). Following the similar procedures of the proof of Proposition 4 in Ref. [20], it can be further proved that Eq. (57) has no other roots except 0, and that Eq. (58) has no root with positive real part for $\alpha \leqslant 1$. Therefore, for $\alpha \leqslant 1$ the partially (fully) locked states are always stable once they emerge for $K \geqslant K_c$, which are in accordance with the numerical observations in Figs. 1, 2, and 3 with $\alpha \leqslant 1$. The instability of partially (fully) locked states is only possible for $\alpha > 1$ caused by the appearance of a positive real root in Eq. (58). As Eq. (58) has only the possibility of real root, the condition for linear stability of the partially (fully) locked states for $\alpha > 1$ can be ultimately stated as

$$h_c(\lambda) \neq \frac{1}{\alpha Kr^{\alpha-1}} \quad \text{for all} \quad \lambda > 0, \tag{59}$$

which has been tested numerically for $\alpha = 2$ with the results in line with Figs. 1(d), 2(d), and 3(d).

The direct integrations of Eq. (57) for $h_s(\lambda)$ and Eq. (58) for $h_c(\lambda)$ turn out to be very difficult for a general $g(w)$. However, using Cauchy's residue theorem [66], both $h_s(\lambda)$ and $h_c(\lambda)$ can be explicitly obtained for the Lorentzian frequency distribution $g(w) = \Delta/\pi(w^2 + \Delta^2)$ as

$$h_s(\lambda) = \frac{1}{2\lambda + Kr^{\alpha-1}} \tag{60}$$

and

$$h_c(\lambda) = \frac{1}{2\lambda + Kr^{\alpha-1} + (1+\alpha)Kr^{\alpha+1}}, \tag{61}$$

for which the detailed calculations are provided in Appendix B. It is obvious from Eq. (60) that $\lambda = 0$ is the only root for Eq. (57). From Eq. (61), it can be inferred that for the appearance of a positive root in Eq. (58), one requires

$$\alpha K r^{\alpha-1} > Kr^{\alpha-1} + (1+\alpha)Kr^{\alpha+1},$$

which is equivalent to

$$r^2 < \frac{\alpha - 1}{\alpha + 1}. \tag{62}$$

Clearly, Eq. (62) fails for $\alpha \leqslant 1$, which holds only possible for $\alpha > 1$. The above analysis indicates that for the Lorentzian frequency distribution $g(w)$, the partially locked states are stable once they are born when $\alpha \leqslant 1$, and are stable only for $r^2 \geqslant \frac{\alpha-1}{\alpha+1}$ if $\alpha > 1$. For $\alpha = 2$, $r = \sqrt{1/3} \approx 0.577$ is predicted at the coupling threshold $K = K_b$, which agrees very well with the numerical observation in Fig. 1(d).

It should be remarked that for $\alpha = 1$, Eqs. (57) and (58) degenerate to the same two characteristic equations obtained previously by Mirollo and Strogatz in Ref. [20], whereas they solved the linear stability of partially (fully) locked states relied on the theory of functional spaces. Here, we have clearly shown that a complete understanding of the spectrum of partially (fully) locked states for Kuramoto-type model can also be achieved from the reduced Ott-Antonsen system with a standard and straightforward method.

IV. CONCLUSIONS

To summarize, we have systematically explored the bifurcation and linear stability of steady states for a variation of Kuramoto model, where the global coupling is modified to depend on the fraction of synchronized oscillators via a power-law function of the Kuramoto order parameter r through an exponent α. The modified phase-model with r-dependent coupling is shown to be analytically tractable in solving both the existence and the linear stability of the steady states for the continuum limit, which degenerates to a standard Kuramoto model in the case of $\alpha = 1$. As $r < 1$, the effective coupling is strengthened if $\alpha < 1$ and weakened if $\alpha > 1$, which result in completely different dynamics of phase transition to synchronization.

Based on a self-consistency analysis in the thermodynamic limit of $N \to \infty$, all the steady states are well characterized by two parametric expressions of the Kuramoto order parameter r and the coupling strength K in Eq. (26). We have found that synchronization diagrams of K versus r for $\alpha < 1$ and $\alpha > 1$ distinctly differ from that of $\alpha = 1$. For $\alpha = 1$, it has been well documented that the partially locked state bifurcates continuously from the incoherent state at $K = K_c = 2/\pi g(0) > 0$, and the second-order phase transition to synchronization is generically reported for strictly unimodal distributions of the natural frequencies such as the Lorentzian and triangle distributions illustrated in Figs. 1(b) and 3(b). One exception is that the first-order phase transition is observed for the uniform frequency distribution in Fig. 2(b), which is due to that the process of partial locking is initiated and completed at the same coupling strength $K = K_c = K_l = 2/\pi g(0)$. However, for $\alpha < 1$, no phase transition is predicted, where the partial locking takes place at $K = K_c = 0$ and the incoherent state is unstable for any $K > 0$. Interestingly, for $\alpha > 1$, the coupling threshold K_c for initial onset of partial locking is found to go to infinity, in contrast to the case of $\alpha \leqslant 1$ with a finite value of K_c. Furthermore, for $\alpha > 1$, we have established an abrupt desynchronization transition from the partially (fully) locked state to the incoherent state at a critical coupling strength $K = K_b$ when adiabatically decreasing K, whereas there is no counterpart of abrupt synchronization transition from incoherence to coherence when progressively increasing K, as the incoherent state is always linearly neutrally stable for all $K > 0$. For $K > K_b$, there exists a bistability between the incoherent state and the partially (fully) locked states.

For each case of α, we have demonstrated that the stability of both the incoherent state and the partially (fully) locked states can be addressed in a similar way by performing a linear stability analysis for the reduced Ott-Antonsen system, despite of the singular nature of the partially locked states. The continuous and discrete spectra are analytically obtained for not only the incoherent state but also the partially (fully) locked states within a uniform framework, from which the linear stability conditions of the corresponding steady states have been derived explicitly. Our work provides a complete framework to investigate the bifurcation and stability of Kuramoto-type systems of globally coupled phase oscillators.

In this work, the Ott-Antonsen ansatz has been employed as a starting point in investigating the stability properties of both the incoherent state and the partially (fully) locked states. However, it is worth to warn that there is no complete guarantee that the Ott-Antonsen ansatz will work, which is due to that the applicability of the Ott-Antonsen ansatz generally requires certain strong assumption, such as the analytic continuations for the oscillator frequency distribution function $g(w)$ to ensure the attraction of Ott-Antonsen manifold [67]. Furthermore, it has been proved that the fairly strong regularity condition should be imposed on the initial phase density for the Ott-Antonsen ansatz to capture the asymptotic behavior of the standard Kuramoto model [68]. Although, the analytic continuations do not hold for the uniform and triangular distributions, our study seems to indicate that the Ott-Antonsen ansatz is perfectly valid in solving both the existence and the linear stability of the steady states of the generalized Kuramoto model with nonlinear coupling in Eq. (3) even for the uniform and triangular frequency distributions. Finally, we hope that the reported results in this paper could be useful for understanding complicated dynamics of phase transitions in complex oscillator networks with nonlinear coupling dependent on the fraction of synchronized subunits.

ACKNOWLEDGMENTS

This work was supported by Research Starting Grants from South China Normal University (Grant No. 8S0340), Guangdong Province Universities and Colleges Pearl River Scholar Funded Scheme (2018), and Natural Science Foundation of Guangdong Province, China (Grant No. 2019A1515011868).

APPENDIX A: VERIFICATION OF THE ROOT IN EQ. (39) FOR PARTIALLY LOCKED STATES

In this Appendix, we provide a self-consistency way to verify that the root $\beta(s)$ in Eq. (39) for the nonzero steady solution of Ott-Antonsen system precisely corresponds to the partially locked states of the continuum model.

First, we show that substitution of the root in Eq. (39) into Eq. (37) yields the same density $f(\theta, w, t)$ of partially locked states in Eq. (11). From Eq. (39), $|\beta(s)| = |is + \sqrt{1-s^2}| = 1$ holds for $|s| \leqslant 1$, corresponding to $|z(t, w)| = 1$ for $|w| \leqslant Kr^\alpha$ as $z(t, w) = \beta(s)$ with $s = w/(Kr^\alpha)$. Thus, the density $f(\theta, w, t)$ in Eq. (37) by inserting $\beta(s)$ for $|s| \leqslant 1$ is

$$f(\theta, w, t) = \delta(\theta - \arg z)g(w),$$

with

$$\arg z = \arg(is + \sqrt{1-s^2}) = \arcsin\left(\frac{w}{Kr^\alpha}\right),$$

which becomes the same to the first part of Eq. (11) with $|w| \leqslant Kr^\alpha$. However, for $|s| > 1$, it is easy to see that $|\beta(s)| = |is(1-\sqrt{1-s^{-2}})| = 1/(|s| + \sqrt{s^2-1}) < 1$, i.e., $|z(t, w)| < 1$ for $|w| > Kr^\alpha$. By substituting $z(t, w) = is(1-\sqrt{1-s^{-2}})$ with $s = w/(Kr^\alpha)$ into Eq. (37), the density $f(\theta, w, t)$ is calculated as

$$\begin{aligned} f(\theta, w, t) &= \frac{g(w)}{2\pi} \frac{(1-|z|)(1+|z|)}{(1-|z|)^2 + 4|z|\sin^2(\frac{\theta - \arg z}{2})} \\ &= \frac{g(w)}{2\pi} \frac{1-|z|^2}{1+|z|^2 - 2|z|\cos(\theta - \arg z)} \\ &= \frac{g(w)}{2\pi} \frac{\sqrt{s^2-1}}{|s| - \mathrm{sgn}(s)\sin\theta} \\ &= \frac{g(w)}{2\pi} \frac{\sqrt{s^2-1}}{\mathrm{sgn}(s)(s - \sin\theta)} \\ &= \frac{g(w)}{2\pi} \frac{\sqrt{w^2 - (Kr^\alpha)^2}}{\mathrm{sgn}(w)(w - Kr^\alpha \sin\theta)}, \end{aligned}$$

which is equivalent to the second part of Eq. (11) with $|w| > Kr^\alpha$.

Second, we demonstrate that the root $\beta(s)$ in Eq. (39) can be obtained from direct computations of the Fourier coefficients in Eq. (33) with the density $f_{\mathrm{PLS}}(\theta, w)$ in Eq. (11). Specifically, for $|w| \leqslant Kr^\alpha$, the corresponding Fourier coefficients are computed as

$$\begin{aligned} z_n(t, w) &= \int_0^{2\pi} e^{in\theta} f(\theta, w, t) d\theta \\ &= \int_0^{2\pi} e^{in\theta} \delta\left(\theta - \arcsin\left(\frac{w}{Kr^\alpha}\right)\right) g(w) d\theta \\ &= \left[i\frac{w}{Kr^\alpha} + \sqrt{1 - \left(\frac{w}{Kr^\alpha}\right)^2} \right]^n g(w) \\ &= \beta^n\left(\frac{w}{Kr^\alpha}\right) g(w), \end{aligned}$$

with

$$\beta(s) = is + \sqrt{1-s^2} \quad \text{for} \quad |s| \leqslant 1. \tag{A1}$$

And for $|w| > Kr^\alpha$, there have

$$\begin{aligned} z_n(t, w) &= \int_0^{2\pi} e^{in\theta} f(\theta, w, t) d\theta \\ &= \int_0^{2\pi} e^{in\theta} \frac{\sqrt{w^2 - (Kr^\alpha)^2}}{2\pi |w - Kr^\alpha \sin\theta|} g(w) d\theta \\ &= C(w) g(w) \int_0^{2\pi} \frac{e^{in\theta}}{w - Kr^\alpha \sin\theta} d\theta, \end{aligned}$$

where $C(w)$ is given in Eq. (16). The above integral can be further computed with the substitution $\gamma = e^{i\theta}$ and Cauchy's residue theorem as

$$\begin{aligned} &\int_0^{2\pi} \frac{e^{in\theta}}{w - Kr^\alpha \sin\theta} d\theta \\ &= \int_{|\gamma|=1} \frac{2\gamma^n}{Kr^\alpha \gamma^2 - i2w\gamma - Kr^\alpha} d\gamma \\ &= \mathrm{sgn}(w) \frac{2\pi \beta^n\left(\frac{w}{Kr^\alpha}\right)}{\sqrt{w^2 - (Kr^\alpha)^2}}, \end{aligned}$$

with

$$\beta(s) = is(1 - \sqrt{1-s^{-2}}) \quad \text{for} \quad |s| > 1. \tag{A2}$$

Thus, for $|w| > Kr^\alpha$, the Fourier coefficients in Eq. (33) become

$$z_n(t, w) = \beta^n\left(\frac{w}{Kr^\alpha}\right) g(w),$$

with $\beta(s)$ given in Eq. (A2). Now, we have that the two expressions for $\beta(s)$ in Eqs. (A1) and (A2) are the same as those in Eq. (39).

Note that from the above calculations, the Fourier series of $f(\theta, w, t)$ in Eq. (11) for partially (fully) locked states has the form of

$$f(\theta, w, t) = \frac{g(w)}{2\pi} \sum_{n=-\infty}^{+\infty} \beta^n\left(\frac{w}{Kr^\alpha}\right) e^{-in\theta}, \tag{A3}$$

which in turn provides a direct indication for Ott-Antonsen ansatz [26,27].

APPENDIX B: $h_c(\lambda)$ and $h_s(\lambda)$ FOR LORENTZIAN FREQUENCY DISTRIBUTION $g(w)$

In this Appendix, we provide the detailed calculations of $h_s(\lambda)$ in Eq. (60) and $h_c(\lambda)$ in Eq. (61) for the Lorentzian frequency distribution

$$g(w) = \frac{\Delta}{\pi(w^2 + \Delta^2)}.$$

Using a contour integration in the complex plane with Cauchy's residue theorem, the order parameter r is computed as

$$\begin{aligned} r &= \int_{-\infty}^{+\infty} z(t,w)g(w)dw = \int_{-\infty}^{+\infty} \beta\left(\frac{w}{Kr^{\alpha}}\right)g(w)dw \\ &= 2\pi i \cdot \mathrm{Res}[\beta\left(\frac{w}{Kr^{\alpha}}\right)g(w), i\Delta] \\ &= 2\pi i \cdot \lim_{w\to i\Delta}(w - i\Delta)\beta\left(\frac{w}{Kr^{\alpha}}\right)g(w) \\ &= \beta\left(\frac{i\Delta}{Kr^{\alpha}}\right), \end{aligned}$$

where $\beta(s)$ satisfies the equation

$$\beta^2(s) - 2is\beta(s) - 1 = 0.$$

Substituting $s = i\Delta/Kr^{\alpha}$ in the above equation of $\beta(s)$ gives

$$Kr^{\alpha+1} - Kr^{\alpha-1} + 2\Delta = 0. \tag{B1}$$

Again, using Cauchy's residue theorem, we have

$$\begin{aligned} J_1(\lambda, r) &= \int_{-\infty}^{+\infty} \frac{(\alpha+1) - (\alpha-1)\beta^2\left(\frac{w}{Kr^{\alpha}}\right)}{\lambda - iw + Kr^{\alpha}\beta\left(\frac{w}{Kr^{\alpha}}\right)}g(w)dw \\ &= \frac{(\alpha+1) - (\alpha-1)\beta^2\left(\frac{i\Delta}{Kr^{\alpha}}\right)}{\lambda - i(i\Delta) + Kr^{\alpha}\beta\left(\frac{i\Delta}{Kr^{\alpha}}\right)} \\ &= \frac{(\alpha+1) - (\alpha-1)r^2}{\lambda + \Delta + Kr^{\alpha+1}} \end{aligned} \tag{B2}$$

and

$$\begin{aligned} J_2(\lambda, r) &= \int_{-\infty}^{+\infty} \frac{(\alpha-1) - (\alpha+1)\beta^2\left(\frac{w}{Kr^{\alpha}}\right)}{\lambda - iw + Kr^{\alpha}\beta\left(\frac{w}{Kr^{\alpha}}\right)}g(w)dw \\ &= \frac{(\alpha-1) - (\alpha+1)\beta^2\left(\frac{i\Delta}{Kr^{\alpha}}\right)}{\lambda - i(i\Delta) + Kr^{\alpha}\beta\left(\frac{i\Delta}{Kr^{\alpha}}\right)} \\ &= \frac{(\alpha-1) - (\alpha+1)r^2}{\lambda + \Delta + Kr^{\alpha+1}}. \end{aligned} \tag{B3}$$

After substituting Eqs. (B2) and (B3) with Eq. (B1) back in Eqs. (55) and (56), we obtain

$$h_s(\lambda) = \frac{1}{2\lambda + Kr^{\alpha-1}}$$

and

$$h_c(\lambda) = \frac{1}{2\lambda + Kr^{\alpha-1} + (1+\alpha)Kr^{\alpha+1}},$$

respectively.

[1] Y. Kuramoto, *Chemical Oscillations, Waves, and Turbulence* (Springer, Berlin, 1984).
[2] A. Pikovsky, M. Rosenblum, and J. Kurths, *Synchronization: A Universal Concept in Nonlinear Sciences* (Cambridge University Press, Cambridge, 2001).
[3] S. H. Strogatz, *Sync: The Emerging Science of Spontaneous Order* (Hyperion, New York, 2003).
[4] Y. Kuramoto, in *International Symposium on Mathematical Problems in Theoretical Physics*, edited by H. Araki, Lecture Notes in Physics, Vol. 39 (Springer, Berlin, 1975).
[5] S. H. Strogatz, Phys. D **143**, 1 (2000).
[6] J. A. Acebrón, L. L. Bonilla, C. J. Pérez Vicente, F. Ritort, and R. Spigler, Rev. Mod. Phys. **77**, 137 (2005).
[7] F. Dörfler and F. Bullo, Automatica **50**, 1539 (2014).
[8] F. A. Rodrigues, T. K. D. M. Peron, P. Ji, and J. Kurths, Phys. Rep. **610**, 1 (2016).
[9] I. Z. Kiss, Y. Zhai, and J. L. Hudson, Science **296**, 1676 (2002).
[10] J. Buck, Quart. Rev. Biol. **63**, 265 (1988).
[11] R. A. Oliva and S. H. Strogatz, Int. J. Bifurcat. Chaos **11**, 2359 (2001).
[12] J. Javaloyes, M. Perrin, and A. Politi, Phys. Rev. E **78**, 011108 (2008).
[13] G. Filatrella, A. H. Nielsen, and N. F. Pedersen, Eur. Phys. J. B **61**, 485 (2008).
[14] M. Rohden, A. Sorge, M. Timme, and D. Witthaut, Phys. Rev. Lett. **109**, 064101 (2012).
[15] F. Dörfler, M. Chertkov, and F. Bullo, Proc. Natl. Acad. Sci. U.S.A. **110**, 2005 (2013).
[16] K. Wiesenfeld and J. W. Swift, Phys. Rev. E **51**, 1020 (1995).
[17] K. Wiesenfeld, P. Colet, and S. H. Strogatz, Phys. Rev. Lett. **76**, 404 (1996).
[18] S. H. Strogatz and R. E. Mirollo, J. Stat. Phys. **63**, 613 (1991).
[19] R. Mirollo and S. H. Strogatz, Phys. D **205**, 249 (2005).
[20] R. Mirollo and S. H. Strogatz, J. Nonlin. Sci. **17**, 309 (2007).
[21] H. Chiba, RIMS Kôkyûroku Bessatsu B **21**, 109128 (2010).
[22] H. Chiba, Ergod. Theory Dyn. Syst. **35**, 762 (2015).
[23] B. Fernandez, D. Gérard-Varet, and G. Giacomin, Ann. Henri Poincare **17**, 1793 (2016).
[24] H. Dietert, J. Math. Pures Appl. **105**, 451 (2016).
[25] H. Dietert and B. Fernandez, Proc. R. Soc. A **474**, 20180467 (2018).
[26] E. Ott and T. M. Antonsen, Chaos **18**, 037113 (2008).
[27] E. Ott and T. M. Antonsen, Chaos **19**, 023117 (2009).
[28] E. A. Martens, E. Barreto, S. H. Strogatz, E. Ott, P. So, and T. M. Antonsen, Phys. Rev. E **79**, 026204 (2009).
[29] D. Pazó and E. Montbrió, Phys. Rev. E **80**, 046215 (2009).
[30] B. Pietras, N. Deschle, and A. Daffertshofer, Phys. Rev. E **94**, 052211 (2016).
[31] B. Pietras, N. Deschle, and A. Daffertshofer, Phys. Rev. E **98**, 062219 (2018).
[32] P. S. Skardal, Phys. Rev. E **98**, 022207 (2018).
[33] Y. Terada, K. Ito, T. Aoyagi, and Y. Y. Yamaguchi, J. Stat. Mech. (2017) 013403.
[34] R. Yoneda and Y. Y. Yamaguchi, J. Stat. Mech. (2020) 033403.
[35] W. S. Lee, E. Ott, and T. M. Antonsen, Phys. Rev. Lett. **103**, 044101 (2009).
[36] P. S. Skardal, Int. J. Bifurcat. Chaos **28**, 01830014 (2018).

[37] D. Métivier and S. Gupta, J. Stat. Phys. **176**, 279 (2019).
[38] H. Hong and S. H. Strogatz, Phys. Rev. Lett. **106**, 054102 (2011).
[39] D. Iatsenko, S. Petkoski, P. V. E. McClintock, and A. Stefanovska, Phys. Rev. Lett. **110**, 064101 (2013).
[40] S. Petkoski, D. Iatsenko, L. Basnarkov, and A. Stefanovska, Phys. Rev. E **87**, 032908 (2013).
[41] C. Xu, J. Gao, H. R. Xiang, W. J. Jia, S. G. Guan, and Z. G. Zheng, Phys. Rev. E **94**, 062204 (2016).
[42] C. Xu, S. Boccaletti, Z. G. Zheng, and S. G. Guan, New J. Phys. **21**, 113018 (2019).
[43] L. Childs and S. H. Strogatz, Chaos **18**, 043128 (2008).
[44] L. F. Lafuerza, P. Colet, and R. Toral, Phys. Rev. Lett. **105**, 084101 (2010).
[45] D. J. Schwab, G. G. Plunk, and P. Mehta, Chaos **22**, 043139 (2012).
[46] W. Zou, M. Zhan, and J. Kurths, Phys. Rev. E **100**, 012209 (2019).
[47] D. M. Abrams, R. Mirollo, S. H. Strogatz, and D. A. Wiley, Phys. Rev. Lett. **101**, 084103 (2008).
[48] T. Kotwal, X. Jiang, and D. M. Abrams, Phys. Rev. Lett. **119**, 264101 (2017).
[49] O. E. Omel'chenko, Nonlinearity **31**, R121 (2018).
[50] O. E. Omel'chenko and M. Wolfrum, Phys. Rev. Lett. **109**, 164101 (2012).
[51] O. E. Omel'chenko and M. Wolfrum, Phys. D **263**, 74 (2013).
[52] O. E. Omel'chenko, M. Sebek, and I. Z. Kiss, Phys. Rev. E **97**, 062207 (2018).
[53] A. Ichiki and K. Okumura, Phys. Rev. E **101**, 022211 (2020).
[54] H. Dietert, B. Fernandez, and D. Gérard-Varet, Commun. Pure. Appl. Math. **71**, 953 (2018).
[55] G. Filatrella, N. F. Pedersen, and K. Wiesenfeld, Phys. Rev. E **75**, 017201 (2007).
[56] M. Rosenblum and A. Pikovsky, Phys. Rev. Lett. **98**, 064101 (2007).
[57] M. Rosenblum and A. Pikovsky, Phys. D **238**, 27 (2009).
[58] F. Giannuzzi, D. Marinazzo, G. Nardulli, M. Pellicoro, and S. Stramaglia, Phys. Rev. E **75**, 051104 (2007).
[59] P. C. Matthews, R. E. Mirollo, and S. H. Strogatz, Phys. D **52**, 293 (1991).
[60] P. S. Skardal and A. Arenas, Phys. Rev. Lett. **122**, 248301 (2019).
[61] P. S. Skardal and A. Arenas, Higher-order interactions in complex networks of phase oscillators promote abrupt synchronization switching, arXiv:1909.08057 (2019).
[62] C. Xu, X. B. Wang, and P. S. Skardal, Phy. Rev. Research **2**, 023281 (2020).
[63] D. Pazó, Phys. Rev. E **72**, 046211 (2005).
[64] L. Basnarkov and V. Urumov, Phys. Rev. E **76**, 057201 (2007).
[65] T. Kato, *Perturbation Theory for Linear Operators* (Springer-Verlag, Berlin, 1995).
[66] M. J. Ablowitz and A. S. Fokas, *Complex Variables: Introduction and Applications* (Cambridge University Press, Cambridge, 2003).
[67] E. Ott, B. R. Hunt, and T. M. Antonsen, Chaos **21**, 025112 (2011).
[68] R. E. Mirollo, Chaos **22**, 043118 (2012).